Identification of *N*-Oxide and Sulfoxide Functionalities in Protonated Drug Metabolites by Using Ion−Molecule Reactions Followed by Collisionally Activated Dissociation in a Linear Quadrupole Ion Trap Mass Spectrometer

Huaming Sheng,[†] Weijuan Tang,[†] Ravikiran Yerabolu,[†] Joann Max,[†] Raghavendhar R. Kotha,[†] James S. Riedeman,[†] John J. Nash,[†] Minli Zhang,[‡] and Hilkka. I. Kenttämaa*,[†]

[†]Purdue University, Department of Chemistry, West Lafayette, Indiana 47907, United States

[‡]AstraZeneca, Boston, Massachusetts 02130, United States

Ⓢ *Supporting Information*

ABSTRACT: The *in vivo* oxidation of sulfur and nitrogen atoms in many drugs into sulfoxide and *N*-oxide functionalities is a common biotransformation process. Unfortunately, the unambiguous identification of these metabolites can be challenging. In the present study, ion−molecule reactions of tris(dimethylamino)borane followed by collisionally activated dissociation (CAD) in an ion trap mass spectrometer are demonstrated to allow the identification of *N*-oxide and sulfoxide functionalities in protonated polyfunctional drug metabolites. Only ions with *N*-oxide or sulfoxide functionality formed diagnostic adducts that had lost dimethyl amine (DMA). This was demonstrated even for an analyte that contains a substantially more basic functionality than the functional group of interest. CAD of the diagnostic product ions (M) resulted mainly in type A (M − DMA) and B fragment ions (M − HO−B(N(CH$_3$)$_2$)$_2$) for *N*-oxides, but sulfoxides also formed diagnostic C ions (M − O=BN(CH$_3$)$_2$), thus allowing differentiation of the functionalities. Some protonated analytes yielded abundant TDMAB adducts that had lost *two* DMA molecules instead of just one. This provides information on the environment of the *N*-oxide and sulfoxide functionalities. Quantum chemical calculations were performed to explore the mechanisms of the above-mentioned reactions. The method can be implemented on HPLC for real drug analysis.
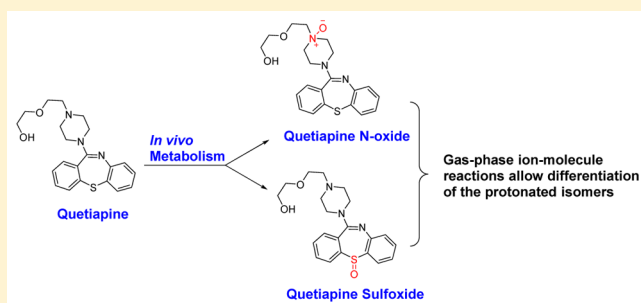
INTRODUCTION

In phase I oxidative metabolism, *N*-oxides and sulfoxides are common metabolites for many sulfur and nitrogen containing heterocyclic drugs[1,2] (for examples of *N*-oxide metabolites,[3] see Figure 1). Fast structural elucidation of these metabolites is essential for the drug discovery process since the metabolites may have profoundly altered functional parameters from those of the drugs, such as adverse biological activity, different clearance rates, and enhanced toxicity.[4−7] Hence, it is crucial to establish methods that allow the unambiguous identification of compounds containing these two functionalities, especially in drugs that contain both sulfur and nitrogen atoms. However, most analytical methods still face challenges in the identification of *N*-oxide and sulfoxide functionalities in molecules in complex mixtures.[8−10]

Although NMR is invaluable in the identification of C-hydroxylation metabolites, the low natural abundances of [15]N (0.37%) and [33]S (0.74%) limit the use of NMR in the detection of N- and S-containing oxidation products.[11,12] Moreover, the metabolite of interest must exist in sufficient quantities and be purified for structure determination by NMR.[13]

Tandem mass spectrometry based on collisionally activated dissociation (CAD) coupled with high-performance liquid chromatography (HPLC/MS/MS) is widely used to identify drug metabolites. However, in many cases, sulfoxide, *N*-oxide, and common C-hydroxylation metabolites have the same molecular weight. Moreover, due to the lack of specific fragmentation patterns for ionized *N*-oxides (for an example, see Figure S1) and sulfoxides upon CAD,[14−16] it is challenging to unambiguously identify these functionalities and to differentiate them from C-hydroxylation metabolites.

Tandem mass spectrometric methods based on ion−molecule reactions hold great promise for being able to provide information useful in the identification of specific functional groups in small organic molecules and in differentiation of isomers.[17−28] This can be carried out on analytes as they elute from an HPLC.[29,30] However, most of these past studies focused on simple monofunctional analytes instead of real polyfunctional drug metabolites. Furthermore, no ion−
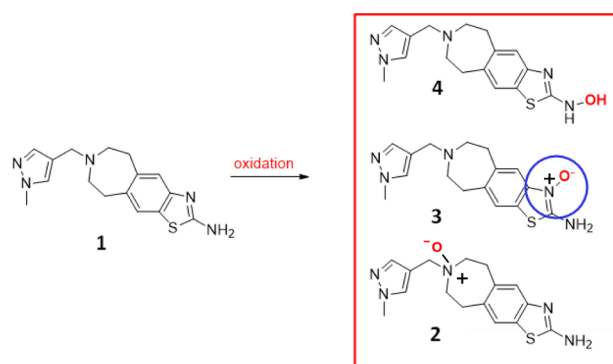
Figure 1. Three possible isomeric oxidation metabolites (2−4) of 2-aminothiazolo-benzazepine (2-ATBA), 7-[(1-methyl-1*H*-pyrazol-4-yl)-methyl]-6,7,8,9-tetrahydro-5*H*-[1,3]thiazolo[4,5-*h*][3]benzazepin-2-amine (1).[3] The *N*-oxides were identified as being formed in human, rat, dog, and monkey microsomes.

molecule reactions have been reported that could be used to differentiate protonated tertiary *N*-oxides from sulfoxides. In the present study, gas-phase ion/molecule reactions of tris(dimethylamino)borane (TDMAB) followed by CAD are demonstrated to allow the unambiguous identification of protonated sulfoxide and *N*-oxide functionalities in polyfunc-

tional drug metabolites. The applicability of the method on a real drug sample was demonstrated by the identification of an *N*-oxide metabolite isolated from dog liver microsomes.

■ RESULTS AND DISCUSSION

Reactions of TDMAB with Protonated Drug Metabolites (MS² Experiments). Protonated monofunctional *N*-oxide, pyridine, and amide model compounds have been reported previously to react with TDMAB via facile formation of a TDMAB adduct that has lost a neutral dimethylamine (DMA) molecule (TDMAB adduct − DMA) in MS² experiments (see the top of Figure 3 for the ion−molecule reaction and a representative MS² spectrum below the mechanism).[24] The same was observed here for the first time for simple sulfoxides (see Table S1 in Supporting Information). Analogous reactivity has *not* been observed for monofunctional compounds containing other functionalities, including sulfide, sulfone, amino, imino, hydroxy, carboxylic acid, and carboxylic ester groups.[24] In this study, formation of a TDMAB adduct followed by elimination of DMA was found to be the major reaction only for protonated polyfunctional drug metabolites containing either an *N*-oxide or a sulfoxide functionality (Figure 2; Table 1). Some *N*-oxides and sulfoxides underwent addition to TDMAB followed by elimination of two DMA molecules instead (discussed later). Other protonated polyfunctional
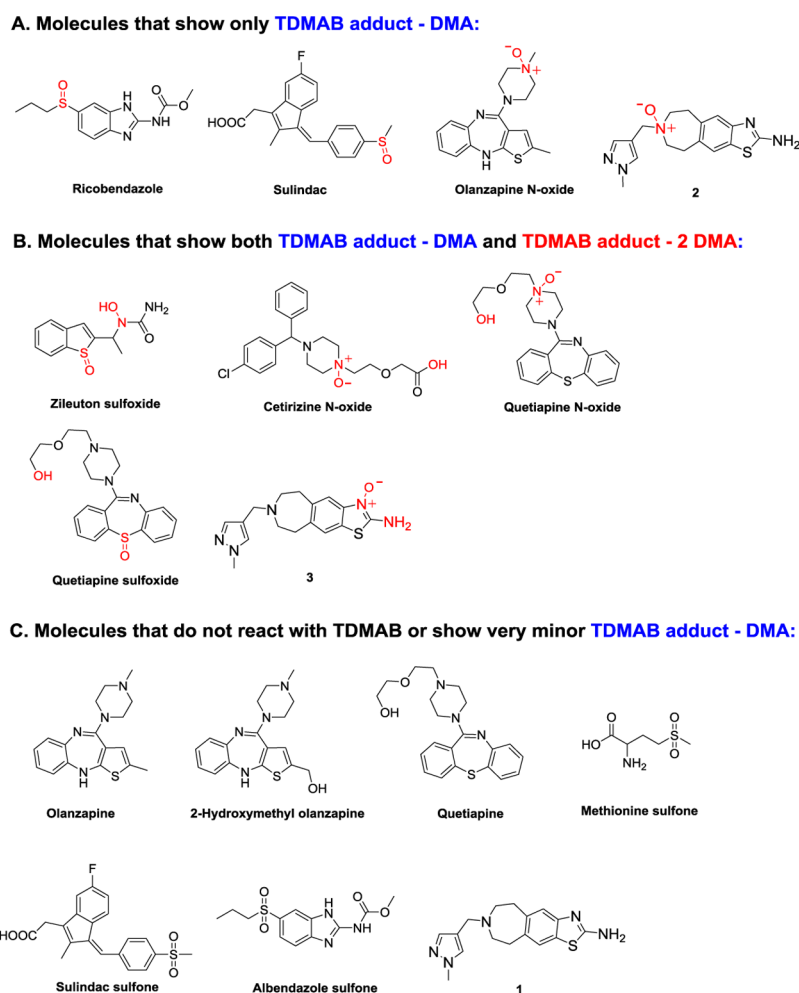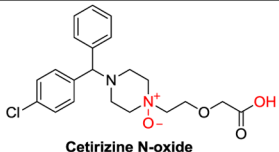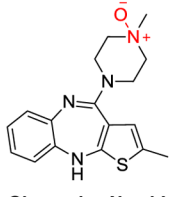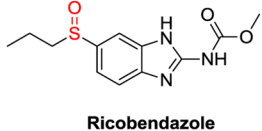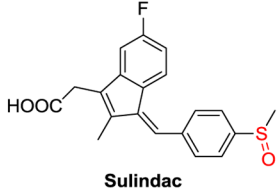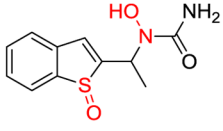

Figure 2. Drugs and drug metabolites used in this study. The functional groups that are involved in the formation of TDMAB adducts that have lost a DMA molecule and TDMAB adducts that have lost two DMA molecules (discussed later in this paper) are marked in red.

Table 1. Observed Product Ions Formed upon Reactions of TDMAB (T) with Protonated Cetirizine N-Oxide, Olanzapine N-Oxide, Ricobendazole, Sulindac and Zileuton Sulfoxide (all referred to as M below) and Their Relative Abundances (MS^2 experiments) as well as the Compositions and Relative Abundances of the CAD Products of the TDMAB Adducts That Had Lost a DMA Molecule (MH$^+$ + T − DMA, also referred to as N below) (MS^3 experiments) (the color coding matches that in Figure 3)

Analyte (M)	Observed product ions and their relative abundances (MS^2)		CAD products of MH$^+$ + T − DMA (N) and their relative abundances (MS^3)
Cetirizine N-oxide	**MH$^+$ + T − 2 DMA (*m/z* 458)**	**45%**	**N − DMA (*m/z* 458) (A) 60%**
	MH$^+$ + T − DMA (*m/z* 503)	**41%**	**N - HOB(N(CH$_3$)$_2$)$_2$ (*m/z* 387)**
	MH$^+$ + DMA^a (*m/z* 450)	14%	**(B) 100%**
Olanzapine N-oxide	**MH$^+$ + T − DMA (*m/z* 427)**	**100%**	**N - DMA (*m/z* 382) (A) 10%**
			N - HOB(N(CH$_3$)$_2$)$_2$ (*m/z* 311)
			(B) 100%
Ricobendazole	**MH$^+$ + T - DMA (*m/z* 380)**	**62%**	**N - DMA (*m/z* 335) (A) 100%**
	MH$^+$ + DMA^a (*m/z* 327)	38%	**N - HOB(N(CH$_3$)$_2$)$_2$ (*m/z* 264)**
			(B) 80%
			N - O=BN(CH$_3$)$_2$ (*m/z* 309)
			(C) 30%
			N- H$_2$O - B(N(CH$_3$)$_2$)$_2$$^+$ (*m/z* 263)
			20%
			T + H$^+$ (m/z 144) 10%
Sulindac	**MH$^+$ + T − DMA (m/z 455)**	**88%**	**N − DMA (*m/z* 410) (A) 20%**
	MH$^+$ (m/z 357)	5%	**N - HOB(N(CH$_3$)$_2$)$_2$ (*m/z* 339)**
	MH$^+$ + DMA^a (m/z 402)	4%	**(B) 50%**
	MH$^+$ + T (m/z 500)	3%	**N - O=BN(CH$_3$)$_2$ (*m/z* 384)**
			(C) 100%
Zileuton Sulfoxide	MH$^+$ + DMA^a (m/z 298)	59%	**N - DMA (*m/z* 306) (A) 100%**
	MH$^+$ + T − DMA (*m/z* 351)	**36%**	**N - O=BN(CH$_3$)$_2$ (*m/z* 280) (C)**
	MH$^+$ + T − 2 DMA (m/z 306)	**5%**	**10%**

^{a}The formation of a DMA adduct upon reaction with TDMAB may occur as shown in Figure S2.

compounds studied (without sulfoxide or *N*-oxide functional groups) did not rapidly undergo either reaction (Figure 2; Table 2).

The likely mechanisms for the formation of TDMAB adducts that have lost a neutral DMA molecule for protonated *N*-oxides and sulfoxides are shown in Figure 3. As proposed in the literature for *N*-oxides,[24] the mechanisms involve initial proton transfer from protonated *N*-oxide or sulfoxide to the amino moiety of TDMAB followed by nucleophilic addition of an oxygen atom of the *N*-oxide or sulfoxide group to the boron center. The proton affinity (PA) of TDMAB is 230 kcal/mol,[24] which is close to the PAs of *N*-oxide[24] (~230 kcal/mol) and sulfoxide[27] (~220 kcal/mol) functionalities in simple analytes. Hence, proton transfer can occur between simple protonated *N*-oxides or sulfoxides and TDMAB, eventually leading to the formation of TDMAB adducts that have lost a DMA molecule.

The selectivity of TDMAB toward protonated *N*-oxides and sulfoxides in simple monofunctional analytes may be partially

Table 2. Observed Product Ions and Their Relative Abundances for Reactions of Protonated Olanzapine, 2-Hydroxymethylolanzapine, Quetiapine, Methionine Sulfone, Sulindac Sulfone, and Albendazole Sulfone (all referred to as M below) (for structures, see Figure 2) with TDMAB (T) (MS[2] experiments)

Analyte (M)	Observed product ions and their relative abundances (MS[2])	
Olanzapine	No Product	
2-Hydroxymethylolanzapine	No Product	
Quetiapine	No Product	
Methionine sulfone	MH$^+$ + DMA^a (m/z 227)	86%
	T + H$^+$ (m/z 144)	14%
	MH$^+$ + DMA^a (m/z 418)	35%
Sulindac sulfone	T + H$^+$ (m/z 144)	34%
	MH$^+$ + T (m/z 516)	26%
	MH$^+$ + T − DMA (m/z 471)	**5%**
Albendazole sulfone	MH$^+$ + DMA^a (m/z 343)	69%
	MH$^+$ + T (m/z 441)	20%
	T + H$^+$ (m/z 144)	7%
	MH$^+$ + T − DMA (m/z 396)	**4%**

^{a}The formation of a DMA adduct upon reaction with TDMAB may occur as shown in Figure S2.

rationalized based on the PAs of the analyte molecules. TDMAB (PA = 230 kcal/mol) readily deprotonates protonated analyte molecules with PAs lower than that of TDMAB, including all analytes with only oxygen-containing functionalities, to yield protonated TDMAB.[24] Protonated sulfones (PAs range from 190−212 kcal/mol[26]) have PAs fairly close to that of TDMAB but lower. Hence, they react with TDMAB to form protonated TDMAB and a stable adduct (Figure 2; Table 2; two sulfones also gave a very small amount of TDMAB adducts that had lost a DMA molecule). As mentioned above, PAs of N-oxide[24] (∼230 kcal/mol) and sulfoxide[27] functionalities (∼220 kcal/mol) in simple compounds are greater than those of sulfones and close to that of TDMAB. This enables formation of a long-lived collision complex after proton transfer, as the proton transfer is not highly exothermic, which would lead to immediate separation of the proton transfer products. Within the long-lived collision complex, nucleophilic addition by the N-oxide[24] or sulfoxide analyte (Table S1) to the boron center of protonated TDMAB can occur and lead to elimination of a DMA molecule as shown in Figure 3.

In order to explore whether the above-mentioned rationale also applies to polyfunctional molecules, quantum chemical calculations were carried out to estimate the PAs of several functionalities in most of the polyfunctional molecules studied (Figures S3−S8), i.e., ricobendazole, albendazole sulfone, quetiapine, quetiapine sulfoxide, quetiapine N-oxide, olanzapine, olanzapine N-oxide, 2-hydroxymethylolanzapine, cetirizine N-oxide, sulindac, sulindac sulfone, methionine sulfone, and compounds 2, 3, and 4 (for structures of these three compounds, see Figure 1). The PAs calculated for all only oxygen- or only sulfur-containing functionalities are less than 210 kcal/mol, as expected. Also as expected, sulfone functionalities were calculated to have similar or slightly greater PAs (199−213 kcal/mol) but still well below that of TDMAB (PA = 230 kcal/mol). Hence, observation of protonated TDMAB and a stable TDMAB adduct for sulindac sulfone, which contains only oxygen- and/or sulfur-containing function-

alities, is not surprising (Table 2). For methionine sulfone and albendazole sulfone, the most basic site is not the sulfone group but a primary amino group and an imino group, respectively. The PAs of these groups (both 222 kcal/mol; Figures S3 and S8) are well below that of TDMAB, which explains the observation of protonated TDMAB and a stable TDMAB adduct also for these protonated molecules (Table 2).

In the other extreme, some analytes, such as quetiapine, olanzapine and hydroxymethylolanzapine, contain a highly basic imino or amino group (the PAs of the most basic tertiary amino groups are 240, 246, and 249 kcal/mol, respectively; Figure S4) that cannot be deprotonated by TDMAB to initiate the diagnostic reaction sequence. Hence, it is not surprising that no reactions were observed for such analytes (quetiapine, olanzapine, and 2-hydroxymethylolanzapine; Table 2).

The diagnostic reactivity (formation of TDMAB adducts that have lost a DMA molecule) dominated only for compounds containing a sulfoxide or an N-oxide functionality. The calculated PAs of the sulfoxide functionalities (219, 224, 230, and 234 kcal/mol) and one N-oxide functionality (231 kcal/mol) in the polyfunctional compounds studied (Figures S3−S8) were found to be similar to those of related simple monofunctional compounds. In most cases, these also are the most basic functionalities in the compounds and thus most likely to be protonated. Hence, it is not surprising that similar reactivity toward TDMAB (Table 1) was observed as in the case of simple monofunctional molecules containing a sulfoxide (Table S1) or an N-oxide[24] functionality. Upon interaction with TDMAB, deprotonation of the protonated N-oxide or sulfoxide functionality occurs and the diagnostic product ion is formed, as shown in Figure 3.

However, the PAs of the N-oxide functionalities in olanzapine N-oxide (240 kcal/mol; Figure S4), cetirizine N-oxide (245 kcal/mol; Figure S5), and quetiapine N-oxide (248 kcal/mol; Figure 4) are very high, likely due to intramolecular hydrogen bond formation with nearby functionalities for two of these analytes (the hydroxyl group 27O in quetiapine N-oxide (Figure 4, bottom) and the carbonyl group 26O in cetirizine N-oxide (Figure S5)). TDMAB should not be able to abstract a proton from these protonated N-oxide groups. In spite of this, the diagnostic TDMAB adducts that had lost a DMA molecule were formed for protonated quetiapine (Table 3), olanzapine and cetirizine N-oxides (Table 1). These findings strongly suggest that the two protonated analytes (ionized by ESI from methanol solution) carry the proton not only on the most basic site (N-oxide) but also on sites with PAs less or equal to that of TDMAB (230 kcal/mol). These sites include a tertiary amino group in quetiapine N-oxide (PA = 218 kcal/mol; Figure 4), in olanzapine N-oxide (PA = 215 kcal/mol; Figure 4) and in cetirizine N-oxide (PA = 223 kcal/mol; Figure S5). The ability of the less basic functionalities to compete for the proton upon ESI may be partially rationalized by the finding that the N-oxide functionalities in neutral quetiapine and cetirizine N-oxides are already involved in stabilizing hydrogen bonding (Figures 3 (top) and S5) and hence may not be accessible for protonation. However, it should be also noted that protonation of other functionalities besides the most basic one upon ESI is not entirely unknown. Gaseous protonated 4-aminobenzoic acid has been reported to carry the proton on either the carbonyl group (favored by 8 kcal/mol in the gas phase) or both the carbonyl group and the amino group, depending on the solvent(s) used.[31a−c] Similarly, 4-hydroxybenzoic acid has been found to be deprotonated on the phenol and/or carboxylic acid
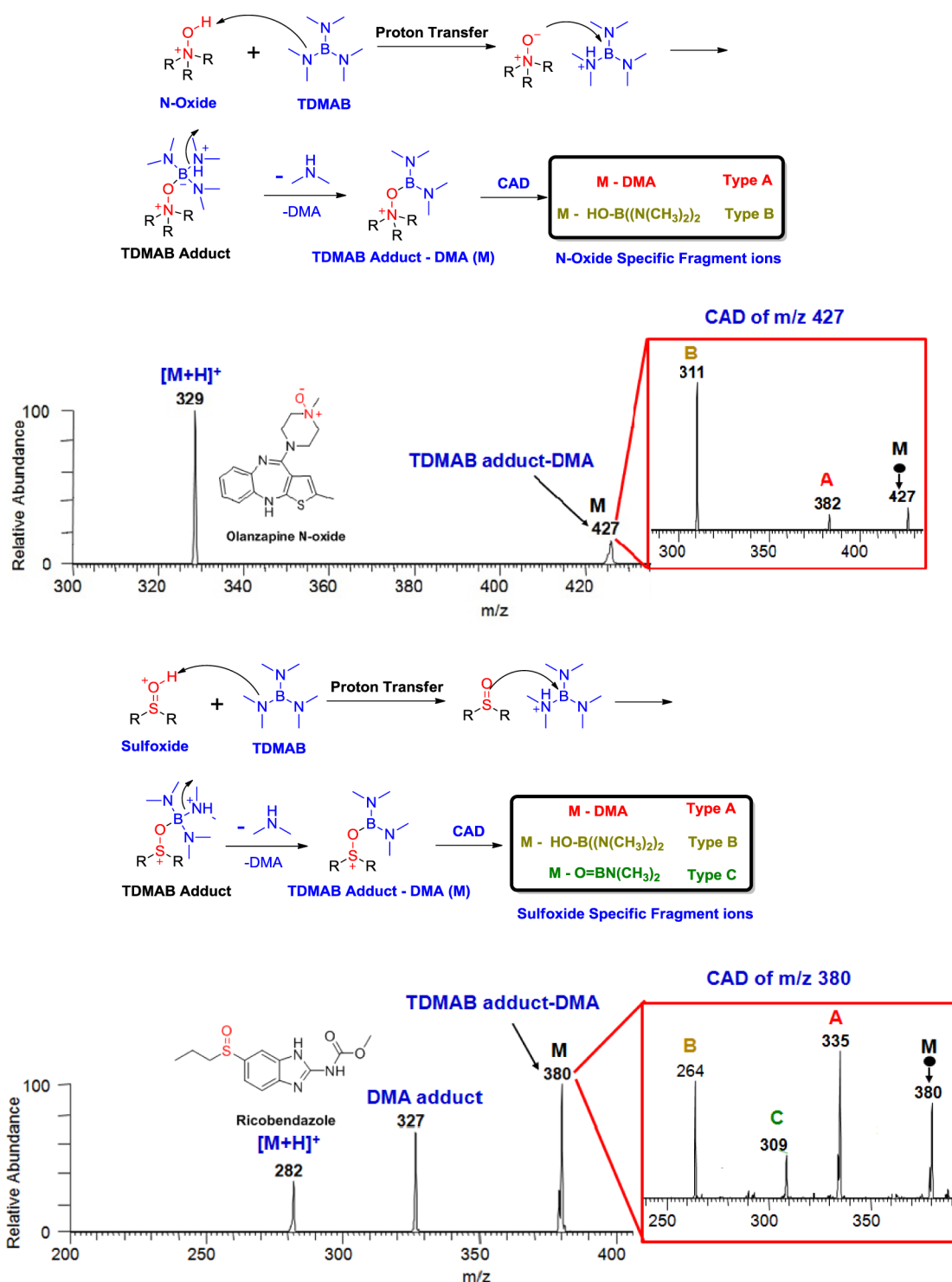
Figure 3. Likely mechanisms leading to the formation of TDMAB adducts that have lost a DMA molecule for protonated *N*-oxides[24] and sulfoxides, MS² spectra showing the products of above reactions, and MS³ CAD mass spectra of the TDMAB adducts that have lost a DMA molecule, illustrated using olanzapine *N*-oxide (top) and ricobendazole (bottom). Only sulfoxides yield the diagnostic type C fragment ions in the MS³ experiment.

sites depending on ESI conditions, in spite of the fact that the phenoxide anion is more stable by 8 kcal/mol in the gas phase.[31d]

Further support for the possibility that the polyfunctional analytes studied here can carry the proton at several sites after ESI is provided by examination of the behavior of one of the sulfoxide-containing analytes. For quetiapine sulfoxide, the sulfoxide group (PA = 234 kcal/mol) is not the most basic site,

as for the other sulfoxides studied; a tertiary amino group and an imino group have substantially greater PAs (245 and 242 kcal/mol, respectively; Figure S4). If this analyte was solely protonated at the most basic amino or imino functionalities, TDMAB could not deprotonate the protonated molecule. However, protonated quetiapine sulfoxide was found to yield the diagnostic TDMAB adduct that had lost a DMA molecule (and a TDMAB adduct that had lost two DMA molecules)
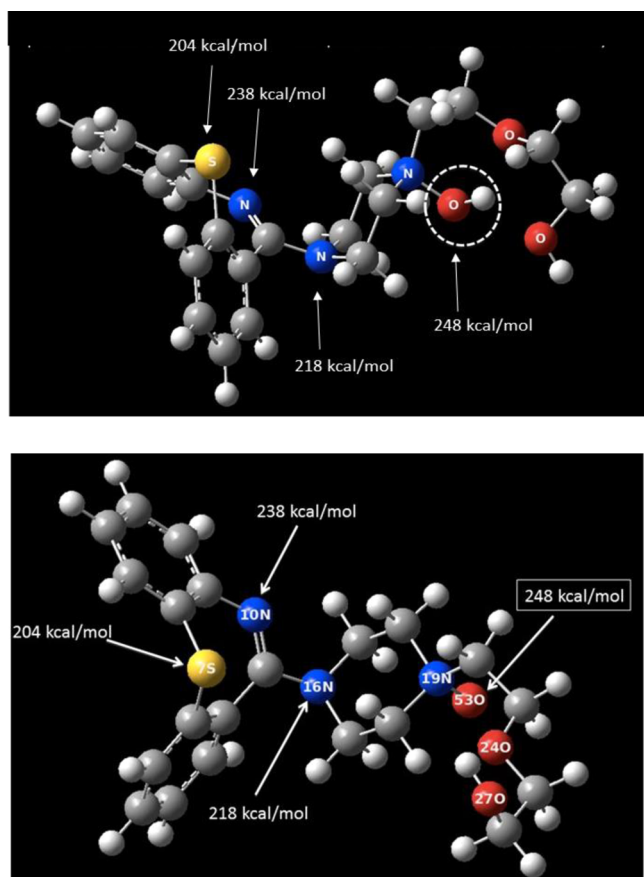
Figure 4. PAs of the most basic functionalities are indicated for the optimized quetiapine *N*-oxide protonated on the *N*-oxide functionality (highlighted with a circle; top) and for the optimized neutral *N*-oxide (bottom; B3LYP/6-31G++(d,p) level of theory). In both structures, the *N*-oxide moiety is involved in hydrogen bonding with the terminal hydroxyl functionality.

(Table 3). Hence, after ESI, this compound must carry a proton at several sites, including the less basic tertiary amino and/or the sulfoxide functionalities (PA = 225 and 234 kcal/mol, respectively; Figure S4).

While the above-mentioned PA considerations help in understanding the behavior of several analytes studied here, they cannot fully explain the selectivity observed for TDMAB. For example, some nitrogen functionalities other than *N*-oxide have PAs close to those of sulfoxides and *N*-oxides, such as, for example, the less basic tertiary amino group (220 kcal/mol) in quetiapine (Figure S4). If this molecule was protonated at this site (in addition to the most basic tertiary amino group with PA = 240 kcal/mol), TDMAB should be able to deprotonate it and form the diagnostic product. However, protonated quetiapine does not form the diagnostic TDMAB adduct that has lost a DMA molecule (Table 2). In agreement with this finding, amines with PAs ranging from 227 up to 242 kcal/mol have been reported to either transfer a proton to TDMAB or be unreactive but not produce TDMAB adducts that have lost a DMA molecule.[24] TDMAB is able to deprotonate protonated amines with PAs below 230 kcal/mol; however, no TDMAB adducts that have lost a DMA molecule were observed for these compounds.

The lack of reactivity of amines toward protonated TDMAB within a collision complex after proton transfer is likely due to their small dipole moments (*e.g.*, those of methyl and triethyl amines are only 1.31 and 0.61 D[32a,b]), which results in only low solvation energy for the proton transfer complex.[33] Hence, the complex is more likely to dissociate to proton transfer products or lose energy upon collisions with helium buffer gas to yield a stable adduct rather than undergo further reactions. On the other hand, the dipole moments of *N*-oxides (that of pyridine *N*-oxide is 4.13 D[31c]) and sulfoxides (that of dimethyl sulfoxide is 3.96 D[31c]) are large. Hence, the proton transfer collision complexes of protonated TDMAB with *N*-oxides and sulfoxides are better stabilized toward dissociation and have longer lifetimes than those of amines, which allows for further reactions within the collision complex after proton transfer.

Collisionally Activated Dissociation (CAD) of the Diagnostic Product Ions (MS³ Experiments). Isolation of the TDMAB adducts that had lost a DMA molecule followed by CAD (MS³ experiments) can be used to differentiate *N*-oxide and sulfoxide containing drug metabolites from each other. For both sulfoxides and *N*-oxides, CAD of the diagnostic ion proceeds through the elimination of a DMA molecule and a $HOB(N(CH_3)_2)_2$ molecule to produce type A and type B fragment ions, respectively (Figure 3; Table 1). However, sulfoxides also produce diagnostic type C fragment ions via elimination of $(CH_3)_2N-B=O$ (Figure 3).
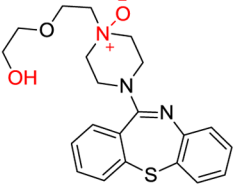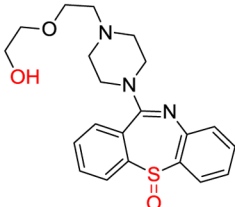
Quantum chemical calculations were used to examine the mechanisms of formation of type A and B fragment ions by using a simple *N*-oxide model compound (Figure 5, left). For type A fragment ions, a six-membered transition state leads to elimination of a DMA molecule. The barrier for formation of type B fragment ions via a different six-membered transition state is calculated to be lower than that for type A ions, in agreement with their relative abundances: type B fragment ions usually dominate (Figure 3; Table 1). These ions are formed via elimination of zwitterionic $O=B^-(N(CH_3)_2)(NH^+(CH_3)_2)$ (Figure 5, bottom left). Based on these calculations, the likely mechanisms for the formation of type A and B fragment ions from the TDMAB adducts that have lost a DMA molecule for protonated olanzapine *N*-oxide are shown in Figure S7.

Further calculations were performed to explore the mechanism of formation of the diagnostic type C fragment ions for sulfoxides by using a simple sulfoxide model compound. A four-membered transition state was found to lead to these fragment ions (Figure 5, right). An analogous mechanism is not possible for *N*-oxides, which explains why they do not form type C fragment ions. Based on calculations, CAD of the TDMAB adduct of sulindac that has lost a DMA molecule likely occurs as shown in Figure 6.

It is interesting to note that CAD of the TDMAB adducts of protonated monofunctional sulfoxide model compounds that have lost a DMA molecule did not show the above-mentioned characteristic fragment ions (Table S1), with the exception of losses of DMA molecules. None of their fragment ions were formed by elimination of a boron containing molecule, as type B and C fragment ions. Instead, they produced either $B(N(CH_3)_2)_2^+$ or $H_2OB(N(CH_3)_2)_2^+$ fragment ions, likely because the N-containing part of the fragmenting ion is able to stabilize the charge better than the sulfoxide-containing part due to its small size. Hence, it is obvious that polyfunctional analytes with an *N*-oxide or sulfoxide functionality can behave very differently from simple compounds.

The formation of type A and B fragment ions via the mechanisms discussed above requires the presence of a hydrogen atom at an atom (carbon for all the compounds discussed above) bound to the sulfoxide or *N*-oxide

Table 3. Observed Ion−molecule Reaction Product Ions and Their Relative Abundances as well as the Compositions and Relative Abundances of the CAD Products of TDMAB Adduct − 2 DMA (MH⁺ + T − 2DMA, also referred to as N below) Formed in Reactions of Protonated Quetiapine N-Oxide and Quetiapine Sulfoxide (referred to as M below) with TDMAB (T)

Analyte (M)	Observed product ions and their relative abundances		CAD of M + T − 2 DMA (N) and the relative abundances of fragment ions
Quetiapine N-oxide	MH⁺ + T − 2 DMA (*m/z* 453) MH⁺ + DMA ᵃ (*m/z* 445) MH⁺ + T − DMA (*m/z* 498)	95% 3% 2%	N − DMA (*m/z* 453)　100% N − O=BN(CH₃)₂ − △ (*m/z* 383) 40%
Quetiapine Sulfoxide	MH⁺ + T − 2 DMA (*m/z* 453) MH⁺ + DMAᵃ (*m/z* 445) MH⁺ + T − DMA (*m/z* 498)	86% 12% 2%	N − O=BN(CH₃)₂ − △ (*m/z* 383) 100%

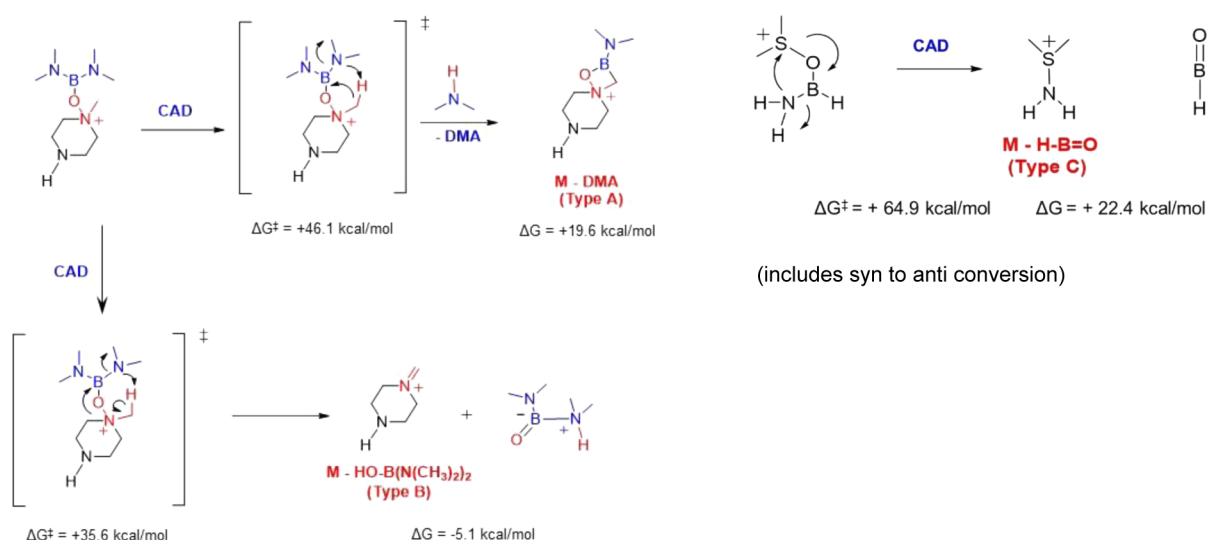ᵃThe formation of a DMA adduct upon reaction with TDMAB may occur as shown in Figure S2.

Figure 5. Calculated free energies of activation and free energy changes for reactions producing type A and B (left) and type C (right) fragment ions for simple model compounds (MØ6-2X/6-311++G(d,p)//MØ6−2X/6-311++G(d,p) level of theory).

functionality. Hence, it is not surprising that no type B ions were observed for zileuton sulfoxide that contains no hydrogen atoms at carbon in the α-position to the sulfoxide group. However, type A fragment ions were nevertheless observed. A possible mechanism for the formation of these ions is shown in Figure 7.

Formation of TDMAB Adducts That Have Lost Two DMA Molecules upon Reactions of Some Protonated Drug Metabolites with TDMAB (MS² Experiments). Some protonated drug metabolites containing a sulfoxide or N-oxide functionality, *i.e.*, cetirizine N-oxide, quetiapine N-oxide, and

quetiapine sulfoxide, showed abundant products due to elimination of not just one but *two* DMA molecules from their TDMAB adducts (TDMAB adduct − 2 DMAB; Tables 1 and 3). These products were not observed for analytes without a sulfoxide or N-oxide functionality. For protonated quetiapine N-oxide and sulfoxide, TDMAB adducts that have lost two DMA molecules are the major product ions (Table 3).

A possible mechanism for the formation of TDMAB adducts of protonated quetiapine that have lost two DMA molecules is shown in Figure 8. After the formation of the TDMAB adduct that has lost one DMA molecule as described above, a hydroxyl
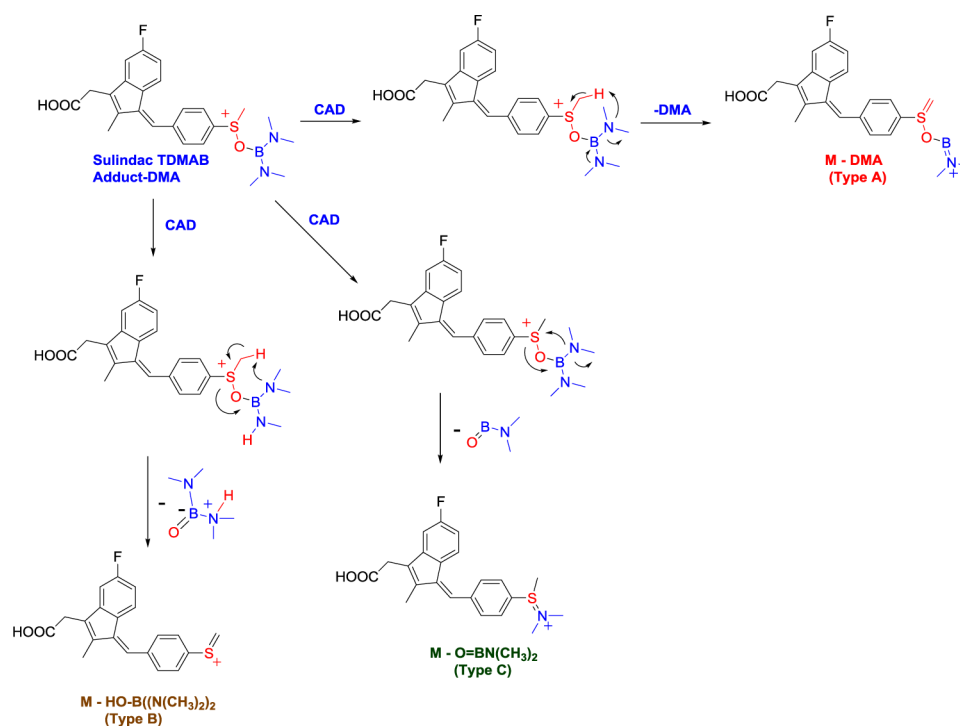
Figure 6. Proposed mechanisms for the formation of type A, B, and C fragment ions from TDMAB adduct of sulindac that has lost a DMA molecule.
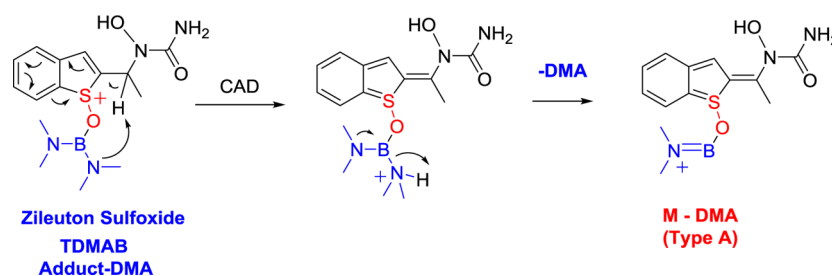

Figure 7. Proposed mechanism for the formation of type A fragment ions upon CAD of TDMAB adduct of zileuton sulfoxide that has lost a DMA molecule.
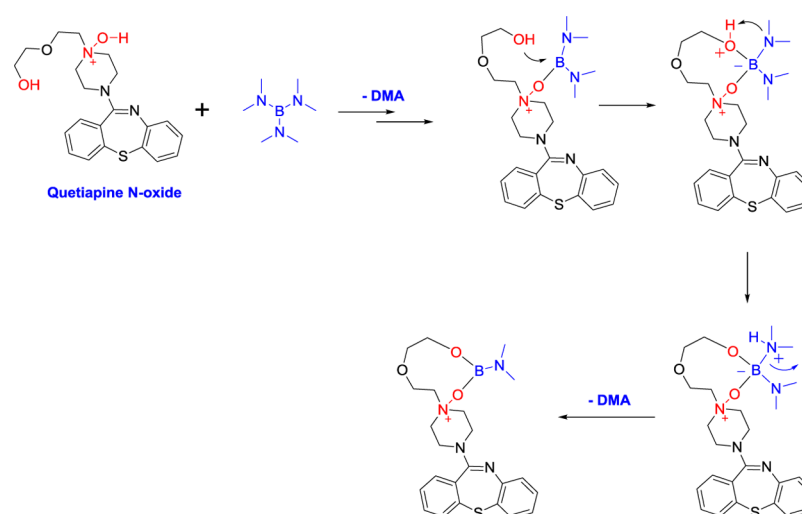

Figure 8. Proposed mechanism for the formation of the TDMAB adducts that have lost two DMA molecules for protonated quetiapine N-oxide.

group in the side chain is likely to add to the boron center, followed by proton transfer and elimination of a second DMA molecule. Formation of analogous product ions by protonated

cetirizine N-oxide and zileuton sulfoxide (Table 1) can be explained in a similar manner by involving nucleophilic attack by their carboxylic acid and hydroxylamino functionalities,
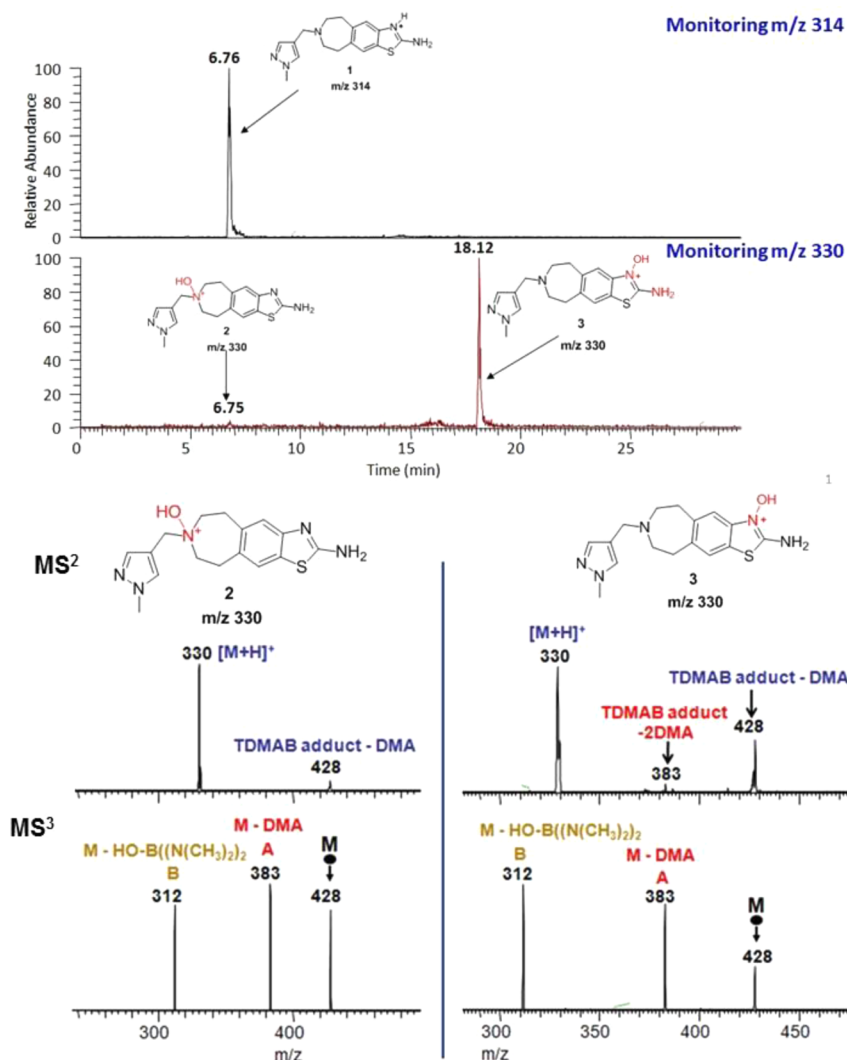
Figure 9. Selected ion chromatograms for ions of m/z 314 and 330 for HPLC separation (phenyl column) of the dog liver metabolite mixture containing compounds **1**−**3** (top) and the MS[2] and MS[3] spectra measured for compounds **2** and **3** ionized by ESI as they eluted from the column (bottom).

respectively. Surprisingly, protonated quetiapine sulfoxide also formed this product ion in spite of not containing a nearby nucleophilic group. It is possible that the hydroxyl functionality in the remote alkyl chain can reach over to the boron atom bound to the sulfoxide group and react as shown in Figure 8 to form TDMAB adducts that have lost two DMA molecules with the calculated structure shown in Figure S8. Support for the structures of the TDMAB adducts that have lost two DMA molecules for quetiapine N-oxide and sulfoxide was obtained by CAD (Figure S11). Based on these results, the observation of TDMAB adducts that have lost two DMA molecules indicates the presence of a sulfoxide or an N-oxide functionality with a nearby nucleophilic group or a nucleophilic group that has access to these functionalities.
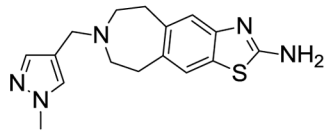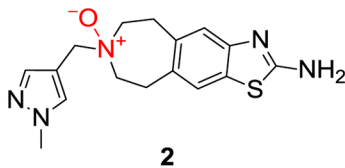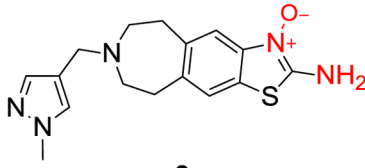
Identification of a Drug Metabolite Isolated from Dog Liver Microsomes. The MS[3] method described above was used to confirm the identification[3] of the drug metabolite **3** shown in Figure 1, an oxidized metabolite of 2-aminothiazolo-benzazepine (**1**). The mass spectrometric characterization of **3** was challenging since CAD only indicated that the oxidation occurred on the thiazole ring.[3] Hence, it was impossible to determine whether the oxidation site was one of the two

nitrogen atoms or the sulfur atom in the thiazole ring (Figure 1; Figure S1). Moreover, compound **3** is labile, which prevented its purification and the synthesis of the metabolite standard. Tandem mass spectrometry and ion−molecule reactions selective for hydroxylamines and N-oxides were used[3] to rule out the hydroxylamine metabolite. Solution reactions were used to rule out the sulfoxide functionality, thus identifying the unknown as the N-oxide **3**. Hence, compound **3** provides a great test case for the proposed MS[3] method that, based on the above-mentioned studies on pure compounds, can be used to differentiate between N-oxide and sulfoxide functionalities in polyfunctional analytes.

Since compound **3** was obtained as a mixture that contains **1**−**3** as well as other metabolites,[3] an HPLC method was first developed to separate **3** from other metabolites. A phenyl column (Figure 9, top) was found to completely separate **3** from the azepine N-oxide **2** whereas a C18 column could not separate these two compounds (Figure S12).

The mass spectrometry results are summarized in Table 4 and Figure 9. The protonated drug molecule **1** did not react with TDMAB, in agreement with the lack of sulfoxide or N-oxide functionalities in this compound. The protonated azepine

Table 4. Observed Ion−Molecule Reaction Product Ions Formed in Reactions of Protonated 1−3 (referred to as M below) with TDMAB (T) and Their Relative Abundances as well as the Compositions and Relative Abundances of the CAD Products of the TDMAB Adducts That Had Lost a DMA Molecule (MH$^+$ + T − DMA, also referred to as N below)

Analyte (M)	Observed product ions and their relative abundances (MS^2)	CAD of TDMAB adduct – DMA (N) and the relative abundances of CAD fragment ions (MS^3)
1	**No Products**	----------
2	**MH$^+$ + T − DMA (*m/z* 428) 100%**	**N − DMA (*m/z* 383) (A) 100%** **N − HOB(N(CH$_3$)$_2$)$_2$ (*m/z* 312) (B) 85%**
3	**MH$^+$ + T − DMA (*m/z* 428) 83%** **MH$^+$ + T − 2 DMA (*m/z* 383) 12%** MH$^+$ + DMA ^{a} (*m/z* 375) 5%	**N − DMA (*m/z* 383) (A) 80%** **N − HOB(N(CH$_3$)$_2$)$_2$ (*m/z* 312) (B) 100%**

^{a}The formation of a DMA adduct upon reaction with TDMAB may occur as shown in Figure S2.

N-oxide reference compound **2** and the unknown metabolite **3** showed the TDMAB adducts that had lost one DMA molecule to be indicative of the presence of a sulfoxide or an *N*-oxide functionality. However, protonated compound **3** also showed the TDMAB adduct that had lost two DMA molecules (Table 4), indicative of an *N*-oxide or sulfoxide with a nearby nucleophilic functionality. This was expected if the oxidized functionality was in the thiazole ring, as suggested earlier based on solution reactions.[3]

Differentiation between sulfoxide and *N*-oxide metabolites was performed using CAD. The TDMAB adducts that had lost a DMA molecule formed from both compounds **2** and **3** gave the typical type A and B fragment ions, as expected. Most importantly, no type C fragment ions diagnostic for a sulfoxide was formed, demonstrating that the unknown compound **3** contains an *N*-oxide functionality. Likely mechanisms for the formation of the TDMAB adducts that have lost a DMA molecule (and those that have lost two DMA molecules) and their CAD reactions are shown in Figures S13 and S14 for **3**. They are analogous to the mechanisms discussed above for pure compounds. In conclusion, the unknown compound was identified as the thiazole *N*-oxide **3** by using HPLC/MS^3 experiments based on ion−molecule reactions and CAD.

■ CONCLUSIONS

In this study, ion−molecule reactions with TDMAB followed by CAD were demonstrated to allow the identification and differentiation of protonated *N*-oxide and sulfoxide containing

drug metabolites in a linear quadrupole ion trap mass spectrometer (Figure 10). Only protonated polyfunctional
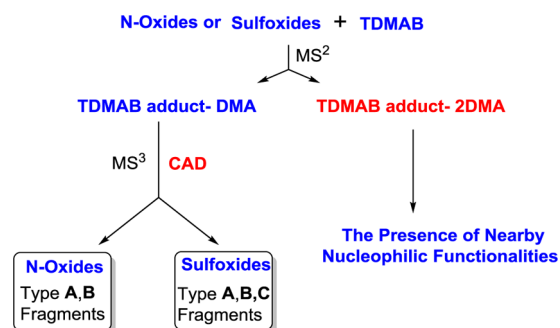
Figure 10. A general scheme for structural characterization of *N*-oxides and sulfoxides by MS^3 experiments employing ion−molecule reactions with TDMAB and CAD.

compounds containing either an *N*-oxide or a sulfoxide functionality showed abundant TDMAB adducts that had lost a DMA molecule (or two DMA molecules) when allowed to react with TDMAB in the gas phase (MS^2 experiments). CAD of the TDMAB adducts that had lost a DMA molecule gave type A and B fragment ions for both sulfoxides and *N*-oxides (MS^3 experiments). However, only sulfoxides yielded diagnostic type C fragment ions, which distinguishes these two functionalities. The formation of TDMAB adducts that have

lost two DMA molecules for some *N*-oxides and sulfoxides in the MS[2] experiments was found to indicate the presence of a nucleophilic group with access to the *N*-oxide or sulfoxide functionality, thus providing information on the chemical environment of these two functional groups (Figure 10). Finally, the ion–molecule reaction/CAD MS[3] method was successfully applied in the identification of a drug metabolite in dog liver microsomes by using HPLC/tandem mass spectrometry.

The results obtained in above studies demonstrated that protonated multifunctional compounds, such as drug metabolites, can carry the proton at several different sites with unequal PAs after evaporation by ESI from methanol solution. Hence, identification of a functionality is possible even when this is not the most basic functionality in the gaseous compound.

■ EXPERIMENTAL SECTION

Materials. Ricobendazole, albendazole, and zioleuton sulfoxide were purchased from Santa Cruz Biotechnology (Dallas, Texas, USA); sulindac and sulindac sulfone were purchased from ENZO Life Sciences (Farmingdale, New York, USA); olanzapine *N*-oxide, 2-hydroxymethylolanzapine, quetiapine, quetiapine *N*-oxide, quetiapine sulfoxide, and cetirizine *N*-oxide were purchased from Toronto Research Chemicals (Toronto, Ontario, Canada); and olanzapine, methionine sulfone, and tris(dimethylamino)borane (TDMAB) were purchased from Sigma-Aldrich (St. Louis, Missouri, USA). High-performance liquid chromatography–mass spectrometry (HPLC/MS) grade water, methanol, and acetonitrile were purchased from Fisher Scientific (Pittsburgh, PA, USA). All chemicals were used without further purification. A Zorbax SB-C18 column (4.6 mm × 250 mm, 5 μm particle size) and a Zorbax SB-Phenyl column (4.6 mm × 250 mm, 5 μm particle size) were purchased from Agilent Technologies (Santa Clara, CA). Compounds **1**–**3** were provided by AstraZeneca. Compound **1** is the parent drug compound. Compound **2** is a synthesized azepine *N*-oxide metabolite of **1**. Compound **3** is the major (unknown) metabolite formed upon incubation of **1** in dog liver microsomes.[3]

Sample Preparation. Stock solutions of all the above-mentioned analytes were prepared at a final concentration of 0.1 mM in methanol. For HPLC/MS analysis, all analytes were dissolved in acetonitrile to achieve a final volume of 1 mL and an analyte concentration of 0.01 mM.

Instrumentation. All mass spectrometry experiments were performed using a Thermo Scientific LTQ linear quadruple ion trap (LQIT) equipped with an ESI source. An integrated syringe drive was used to directly infuse the analyte solutions into the ESI source at a rate of 20 μL/min. All analytes were ionized via (+) ESI. The (+) ESI conditions were as follows: 3.5–4 kV spray voltage, sheath and auxiliary gas (N_2) flow of 20 and 10 (arbitrary units), and a heated ion transfer capillary/mass spectrometer inlet temperature of 275 °C. The voltages for the ion optics were optimized for each analyte by using the tune feature of the LTQ Tune Plus interface. The protonated, isolated analytes were allowed to react with the reagent TDMAB in the ion trap for 50 up to 500 ms; however, up to 1000 ms were used in cases where no reactions were observed.

The manifold used to introduce reagents into the helium buffer gas line was first described by Gronert.[34,35] A diagram of the exact manifold used in this research was published by Habicht et al.[19] TDMAB was introduced into the manifold via a syringe pump at a flow rate of 20 μL/h. A known amount of He (1.5 L/h) was used to dilute TDMAB. The syringe port and surrounding area were heated to ~90 °C to ensure evaporation of TDMAB. Before entering the trap, the He/reagent mixture was split using two Granville-Phillips leak valves, instead of the standard flow splitter. This allowed better control over the amount of the mixture introduced into the instrument. One leak valve was set to establish a helium pressure of ~3 m Torr in the ion trap by allowing ~2 mL/min of the mixture into the trap[36] while the other leak valve controlled the amount of flow diverted to waste. A

typical nominal pressure of TDMAB in the trap during the experiments was 0.68×10^{-5} Torr. After the experiments were completed each day, the manifold was isolated from the instrument and placed under vacuum to remove any remaining reagent.

In collisionally activated dissociation (CAD) experiments, the advanced scan features of the LTQ Tune Plus interface were used to isolate the ions by using an *m/z* window of 2 units. At a *q* value of 0.25, the ions were subjected to CAD by using helium as the collision gas for an activation time of 30 ms. "Normalized collision energies" were varied from 20% up to 40%.

The detection mass range was from *m/z* 50 up to 500. All mass spectra acquired were an average of at least 20 spectra. Xcalibur 2.0 software was used for processing of all data produced.

High Performance Liquid Chromatography/Tandem Mass Spectrometry. The reference compounds **1** and **2** and the dog liver metabolite mixture of **1** (obtained as described in the literature[3]) were introduced into the HPLC/MS via an autosampler as a full-loop injection volume for high reproducibility. The flow rate was 0.5 mL/min. Solutions containing 0.1% (v/v) formic acid in water (A) and 0.1% formic acid (v/v) in acetonitrile (B) were used as the mobile phase solvents. Formic acid was chosen to encourage positive ion production. The nonlinear gradient used was as follows: 0.0 min, 95% A and 5% B; 10.0 min, 80% A and 20% B; 18.0 min, 55% A and 45% B; 25.0 min, 3% A and 97% B; 26.0 min, 3% A and 97% B; 26.1 min, 95% A and 5% B; 30.0 min, 95% A and 5% B. The column was located in a thermostated compartment where the temperature was maintained at 30 °C. Mass spectrometric analysis of the HPLC eluent was performed using single ion monitoring for ions of *m/z* 314 (protonated **1**) and *m/z* 330 (protonated **2** and **3**). Ions with the *m/z* values 314 and *m/z* 330 were selected for further isolation and MS[2] experiments involving CAD. For MS[2] experiments, an ion isolation window of 2 *m/z* was used prior to ion fragmentation at a *q* value of 0.25 for 30 ms at a normalized collision energy of 35% (arbitrary units).

Computational Studies. The Gaussian 03 suite of programs was used for all calculations.[37] Proton affinities were calculated at the B3LYP/6-31G++(d,p) level of theory. All the neutral and protonated molecules' lowest energy conformers were identified using the Maestro 7.0 Macro-model conformational search. The free energies of activation and reaction were calculated at the MØ6-2X/6-311++G(d,p)//MØ6-2X/6-311++G(d,p) level of theory.

■ ASSOCIATED CONTENT

Ⓢ Supporting Information

The Supporting Information is available free of charge on the ACS Publications website at DOI: 10.1021/acs.joc.5b02409.

Minimum energy geometry data (ZIP)

Additional information on the proton affinity and potential energy surface calculations of some molecules, HPLC chromatogram of C18 column for separation of the mixture of **3** and the ion–molecule reaction results of TDMAB with some simple sulfoxide model compounds (PDF)

■ AUTHOR INFORMATION

Corresponding Author
*E-mail: hilkka@purdue.edu.

Notes

The authors declare no competing financial interest.

■ ACKNOWLEDGMENTS

■ REFERENCES

(1) (a) Crettol, S.; Petrovic, N.; Murray, M. *Curr. Pharm. Des.* **2010**, *16*, 204−219. (b) Zuniga, F. I.; Loi, D.; Ling, K. H.; Tang-Liu, D. D. *Expert Opin. Drug Metab. Toxicol.* **2012**, *8*, 467−485.

(2) Chen, X.; Hussain, S.; Parveen, S.; Zhang, S.; Yang, Y.; Zhu, C. *Curr. Med. Chem.* **2012**, *19*, 3578−3604.

(3) Zhang, M.; Eismin, R.; Kenttämaa, H. I.; Xiong, H.; Wu, Y.; Burdette, D.; Urbanek, R. *Drug Metab. Dispos.* **2015**, *43*, 358−366.

(4) Bright, T. V.; Dalton, F.; Elder, V. L.; Murphy, C. D.; O'Connor, N. K.; Sandford, G. *Org. Biomol. Chem.* **2013**, *11*, 1135−1142.

(5) St. Jean, D. J., Jr.; Fotsch, C. *J. Med. Chem.* **2012**, *55*, 6002−6020.

(6) Park, B. K.; Boobis, A.; Clarke, S.; Goldring, C. E. P.; Jones, D.; Kenna, J. G.; Lambert, C.; Laverty, H. G.; Naisbitt, D. J.; Nelson, S.; Nicoll-Griffith, D. A.; Obach, R. S.; Routledge, P.; Smith, D. A.; Tweedie, D. J.; Vermeulen, N.; Williams, D. P.; Wilson, I. D.; Baillie, T. A. *Nat. Rev. Drug Discovery* **2011**, *10*, 292−306.

(7) Kalgutkar, A. S.; Gardner, I.; Obach, R. S.; Shaffer, C. L.; Callegari, E.; Henne, K. R.; Mutlib, A. E.; Dalvie, D. K.; Lee, J. S.; Nakai, Y.; O'Donnell, J. P.; Boer, J.; Harriman, S. P. *Curr. Drug Metab.* **2005**, *6*, 161−225.

(8) Caslavska, J.; Thormann, W. *J. Chromatogr. A* **2011**, *1218*, 588−601.

(9) Bhave, D. P.; Muse, W. B., 3rd; Carroll, K. S. *Infect. Disord.: Drug Targets* **2007**, *7*, 140−158.

(10) Dibbern, D. A., Jr.; Montanaro, A. *Ann. Allergy, Asthma, Immunol.* **2008**, *100*, 91−100.

(11) Prakash, C.; Shaffer, C. L.; Nedderman, A. *Mass Spectrom. Rev.* **2007**, *26*, 340−369.

(12) Palmnas, M. S.A.; Vogel, H. J. *Metabolites* **2013**, *3*, 373−396.

(13) Lenz, E. M. *Methods Mol. Biol.* **2011**, *708*, 299−319.

(14) Froelich, J. M.; Reid, G. E. *J. Am. Soc. Mass Spectrom.* **2007**, *18*, 1690−1705.

(15) Reid, G. E.; Roberts, K. D.; Kapp, E. A.; Simpson, R. I. *J. Proteome Res.* **2004**, *3*, 751−759.

(16) Jiang, X.; Smith, J. B.; Abraham, E. C. *J. Mass Spectrom.* **1996**, *31*, 1309−1310.

(17) Osburn, S.; Ryzhov, V. *Anal. Chem.* **2013**, *85*, 769−778.

(18) Eismin, R. J.; Fu, M.; Yem, S.; Widjaja, F.; Kenttämaa, H. I. *J. Am. Soc. Mass Spectrom.* **2012**, *23*, 12−22.

(19) Habicht, S. C.; Vinueza, N. R.; Archibold, E. F.; Duan, P.; Kenttämaa, H. I. *Anal. Chem.* **2008**, *80*, 3416−3421.

(20) Campbell, K. M.; Watkins, M. A.; Li, S.; Fiddler, M. N.; Winger, B.; Kenttämaa, H. I. *J. Org. Chem.* **2007**, *72*, 3159−3165.

(21) Somuramasami, J.; Duan, P.; Amundson, L.; Archibold, E.; Winger, B.; Kenttämaa, H. I. *J. Am. Soc. Mass Spectrom.* **2011**, *22*, 1040−1051.

(22) Fu, M.; Eismin, R. J.; Duan, P.; Li, S.; Kenttämaa, H. I. *Int. J. Mass Spectrom.* **2009**, *282*, 77−84.

(23) Fu, M.; Duan, P.; Li, S.; Habicht, S. C.; Pinkston, D. S.; Vinueza, N. R.; Kenttämaa, H. I. *Analyst* **2008**, *133*, 452−454.

(24) Duan, P.; Fu, M.; Gillespie, T. A.; Winger, E.; Kenttämaa, H. I. *J. Org. Chem.* **2009**, *74*, 1114−1123.

(25) Duan, P.; Gillespie, T. A.; Winger, B. E.; Kenttämaa, H. I. *J. Org. Chem.* **2008**, *73*, 4888−4894.

(26) Sheng, H.; Williams, P. E.; Tang, W.; Riedeman, J. S.; Zhang, M.; Kenttämaa, H. I. *J. Org. Chem.* **2014**, *79*, 2883−2889.

(27) Sheng, H.; Williams, P. E.; Tang, W.; Zhang, M.; Kenttämaa, H. I. *Analyst* **2014**, *139*, 4296−4302.

(28) Sheng, H.; Tang, W.; Yerabolu, R.; Kong, J. Y.; Williams, P. E.; Zhang, M.; Kenttämaa, H. I. *Rapid Commun. Mass Spectrom.* **2015**, *29*, 730−734.

(29) Habicht, S. C.; Vinueza, N. R.; Amundson, L. M.; Kenttämaa, H. I. *J. Am. Soc. Mass Spectrom.* **2011**, *22*, 520−530.

(30) Habicht, S. C.; Duan, P.; Vinueza, N. R.; Fu, M.; Kenttämaa, H. I. *J. Pharm. Biomed. Anal.* **2010**, *51*, 805−811.

(31) (a) Tian, Z.; Kass, S. R. *Angew. Chem., Int. Ed.* **2009**, *48*, 1321−1323. (b) Schmidt, J.; Meyer, M. K.; Spector, I.; Kass, S. R. *J. Phys. Chem. A* **2011**, *115*, 7625−7632. (c) Campbell, J. L.; Le Blanc, J. C. Y.; Schneider, B. B. *Anal. Chem.* **2012**, *84*, 7857−7864. (d) Schröder, D.; Budĕšínský, M.; Roithová, J. *J. Am. Chem. Soc.* **2012**, *134*, 15897−15905.

(32) (a) Nelson, R. D., Lide, D. R., Maryott, A. A. *National Standard Reference Data Series-National Bureau of Standards 10*. Washington, DC, 20402 (retrieved May 10, 2015). (b) Pople, J. A.; Gordon, M. *J. Am. Chem. Soc.* **1967**, *89*, 4253−4261. (c) Brown, R. D.; Burden, F. R.; Garland, W. *Chem. Phys. Lett.* **1970**, *7*, 461−462.

(33) Bowers, M. T. *Gas Phase Ion Chemistry*, Vol. 1; Academic Press: 1979.

(34) Gronert, S. *J. Am. Soc. Mass Spectrom.* **1998**, *9*, 845−848.

(35) Gronert, S. *Mass Spectrom. Rev.* **2005**, *24*, 100−120.

(36) Schwartz, J. C.; Senko, M. W.; Syka, J. E. *J. Am. Soc. Mass Spectrom.* **2002**, *13*, 659−669.

(37) Frisch, M. J.; Trucks, G. W.; Schlegel, H. B.; Scuseria, G. E.; Robb, M. A.; Cheeseman, J. R.; Montgomery, Jr., J. A.; Vreven, T.; Kudin, K. N.; Burant, J. C.; Millam, J. M.; Iyengar, S. S.; Tomasi, J.; Barone, V.; Mennucci, B.; Cossi, M.; Scalmani, G.; Rega, N.; Petersson, G. A.; Nakatsuji, H.; Hada, M.; Ehara, M.; Toyota, K.; Fukuda, R.; Hasegawa, J.; Ishida, M.; Nakajima, T.; Honda, Y.; Kitao, O.; Nakai, H.; Klene, M.; Li, X.; Knox, J. E.; Hratchian, H. P.; Cross, J. B.; Bakken, V.; Adamo, C.; Jaramillo, J.; Gomperts, R.; Stratmann, R. E.; Yazyev, O.; Austin, A. J.; Cammi, R.; Pomelli, C.; Ochterski, J. W.; Ayala, P. Y.; Morokuma, K.; Voth, G. A.; Salvador, P.; Dannenberg, J. J.; Zakrzewski, V. G.; Dapprich, S.; Daniels, A. D.; Strain, M. C.; Farkas, O.; Malick, D. K.; Rabuck, A. D.; Raghavachari, K.; Foresman, J. B.; Ortiz, J. V.; Cui, Q.; Baboul, A. G.; Clifford, S.; Cioslowski, J.; Stefanov, B. B.; Liu, G.; Liashenko, A.; Piskorz, P.; Komaromi, I.; Martin, R. L.; Fox, D. J.; Keith, T.; Al-Laham, M. A.; Peng, C. Y.; Nanayakkara, A.; Challacombe, M.; Gill, P. M. W.; Johnson, B.; Chen, W.; Wong, M. W.; Gonzalez, C.; Pople, J. A. *Gaussian 03*, Revision C.02; Gaussian, Inc.: Wallingford, CT, 2004.